Modelling and Identification of Immune Cell Migration during the Inflammatory Response

PhD Viva (extended version)

A. Kadochnikova[1]

[1]Department of Automatic Control and Systems Engineering
The University of Sheffield

June 24, 2019

Outline

Experimental studies ⟷ Mathematical models

Experimental studies

Recruitment
via chemotaxis

Mathematical models

Experimental studies

Recruitment
via chemotaxis

in vivo microscopy
on zebrafish larvae

Mathematical models

Experimental studies

Recruitment via chemotaxis

in vivo microscopy on zebrafish larvae

Resolution via reverse migration

Mathematical models

Experimental studies

- Recruitment via chemotaxis
- *in vivo* microscopy on zebrafish larvae
- Resolution via reverse migration
- Sensing to motion via subcellular signals

Mathematical models

Experimental studies

Recruitment
via chemotaxis

in vivo microscopy
on zebrafish larvae

Resolution via
reverse migration

Sensing to motion
via subcellular signals

Mathematical models

RDS models
for populations

Experimental studies

- Recruitment via chemotaxis
- *in vivo* microscopy on zebrafish larvae
- Resolution via reverse migration
- Sensing to motion via subcellular signals

↔

Mathematical models

- RDS models for populations
- Random walk models for single cells

Experimental studies

- Recruitment via chemotaxis
- *in vivo* microscopy on zebrafish larvae
- Resolution via reverse migration
- Sensing to motion via subcellular signals

↔

Mathematical models

- RDS models for populations
- Random walk models for single cells
- RDS models for subcellular species

Experimental studies

- Recruitment via chemotaxis
- *in vivo* microscopy on zebrafish larvae
- Resolution via reverse migration
- Sensing to motion via subcellular signals

↔

Mathematical models

- RDS models for populations
- Random walk models for single cells
- RDS models for subcellular species
- Morphodynamics as intermediate level

Experimental studies

- Recruitment via chemotaxis
- *in vivo* microscopy on zebrafish larvae
- Resolution via reverse migration
- Sensing to motion via subcellular signals

!!!

Mathematical models

- RDS models for populations
- Random walk models for single cells
- RDS models for subcellular species
- Morphodynamics as intermediate level

Experimental studies

- Recruitment via chemotaxis
- Environment unobserved
- Resolution via reverse migration
- Sensing to motion via subcellular signals

!!!

Mathematical models

- RDS models for populations
- Random walk models for single cells
- RDS models for subcellular species
- Morphodynamics as intermediate level

Experimental studies

Recruitment via chemotaxis

Environment unobserved

Random walk or fugetaxis?

Sensing to motion via subcellular signals

!!!

Mathematical models

RDS models for populations

Random walk models for single cells

RDS models for subcellular species

Morphodynamics as intermediate level

Experimental studies

Recruitment via chemotaxis

Environment unobserved

Random walk or fugetaxis?

Sensing to motion via subcellular signals

!!!

Mathematical models

RDS models for populations

RWs do not reflect global environent

RDS models for subcellular species

Morphodynamics as intermediate level

Experimental studies

Recruitment via chemotaxis

Environment unobserved

Random walk or fugetaxis?

Sensing to motion via subcellular signals

!!!

Mathematical models

RDS models for populations

RWs do not reflect global environent

Models not informed by experimental data

Common concept:
Complicated model $\rightarrow$ Realistic simulations.

Systematic approach:
Simplified models $\rightarrow$ Linking to data $\rightarrow$ Meaningful perditions.

Systematic approach:
Simplified models $\rightarrow$ Linking to data $\rightarrow$ Meaningful perditions.

Objectives:

- Develop a dynamical model that describes cell interaction with the global environment.
- Data-driven estimation of global chemoattractant concentration and cell behavioural modes.
- Parameter estimation of neutrophil morphodynamics model.

Hidden chemoattractant

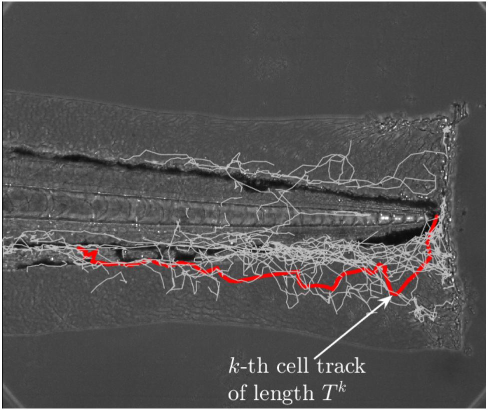

Time series data:

- K tracks: $\mathcal{Y} = \{\mathbf{y}^k\}_{k=1}^{K}$
- Single track:
  $\mathbf{y}^k = \{y_t^k\}_{t=1}^{T^k}$
- Single data point:
  $y_t^k = \left[\bar{s}_{\mathrm{x}}, \bar{s}_{\mathrm{y}}\right]^\top$
- Full state:
  $x_t^k = \left[s_{\mathrm{x}}, s_{\mathrm{y}}, v_{\mathrm{x}}, v_{\mathrm{y}}\right]^\top$
- Environment influence:
  $u_t^k = u_t^k(s) = \nabla \mathcal{U}(s)$.

Hidden chemoattractant

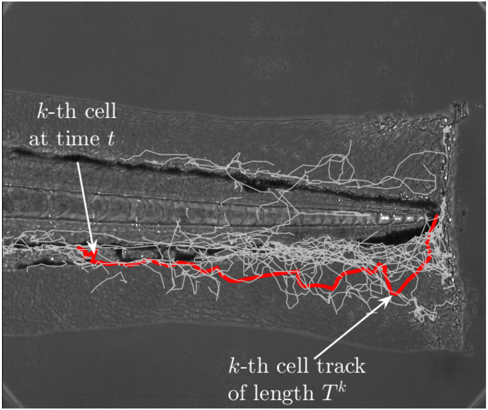

Time series data:

- K tracks: $\mathcal{Y} = \{\mathbf{y}^k\}_{k=1}^{K}$
- Single track: $\mathbf{y}^k = \{\boldsymbol{y}_t^k\}_{t=1}^{T^k}$
- Single data point: $\boldsymbol{y}_t^k = [\bar{s}_\mathrm{x}, \bar{s}_\mathrm{y}]^\top$
- Full state: $\boldsymbol{x}_t^k = [s_\mathrm{x}, s_\mathrm{y}, v_\mathrm{x}, v_\mathrm{y}]^\top$
- Environment influence: $\boldsymbol{u}_t^k = \boldsymbol{u}_t^k(\boldsymbol{s}) = \nabla\mathcal{U}(\boldsymbol{s})$.

Hidden chemoattractant

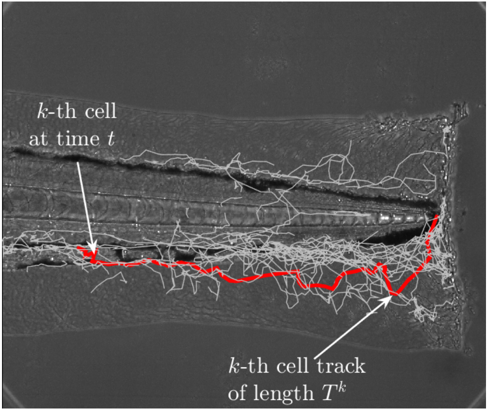

Time series data:

- K tracks: $\mathcal{Y} = \{\mathbf{y}^k\}_{k=1}^K$
- Single track: $\mathbf{y}^k = \{\boldsymbol{y}_t^k\}_{t=1}^{T^k}$
- Single data point: $\boldsymbol{y}_t^k = \left[\bar{s}_\mathrm{x}, \bar{s}_\mathrm{y}\right]^\top$
- Full state: $\boldsymbol{x}_t^k = \left[s_\mathrm{x}, s_\mathrm{y}, v_\mathrm{x}, v_\mathrm{y}\right]^\top$
- Environment influence: $\boldsymbol{u}_t^k = \boldsymbol{u}_t^k(\boldsymbol{s}) = \nabla\mathcal{U}(\boldsymbol{s})$.

Hidden chemoattractant

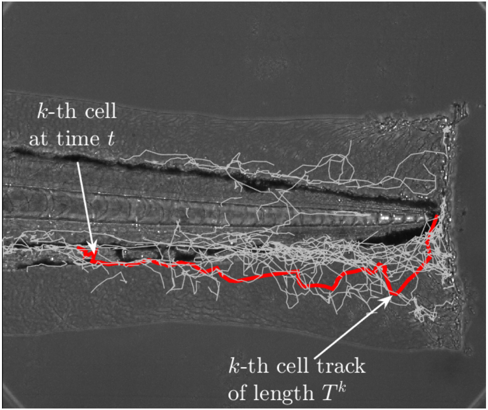

Time series data:

- K tracks: $\mathcal{Y} = \{\mathbf{y}^k\}_{k=1}^{K}$
- Single track:
  $\mathbf{y}^k = \{\boldsymbol{y}_t^k\}_{t=1}^{T^k}$
- Single data point:
  $\boldsymbol{y}_t^k = \left[\bar{s}_x, \bar{s}_y\right]^\top$
- Full state:
  $\boldsymbol{x}_t^k = \left[s_x, s_y, v_x, v_y\right]^\top$
- Environment influence:
  $\boldsymbol{u}_t^k = \boldsymbol{u}_t^k(\boldsymbol{s}) = \nabla\mathcal{U}(\boldsymbol{s})$.

Hidden chemoattractant

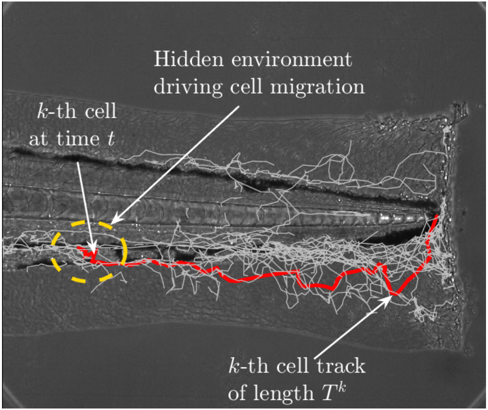

Time series data:

- K tracks: $\mathcal{Y} = \{\mathbf{y}^k\}_{k=1}^K$
- Single track:
  $\mathbf{y}^k = \{\boldsymbol{y}_t^k\}_{t=1}^{T^k}$
- Single data point:
  $\boldsymbol{y}_t^k = \left[\bar{s}_{\mathrm{x}}, \bar{s}_{\mathrm{y}}\right]^\top$
- Full state:
  $\boldsymbol{x}_t^k = \left[s_{\mathrm{x}}, s_{\mathrm{y}}, v_{\mathrm{x}}, v_{\mathrm{y}}\right]^\top$
- Environment influence:
  $\boldsymbol{u}_t^k = \boldsymbol{u}_t^k(\boldsymbol{s}) = \nabla\mathcal{U}(\boldsymbol{s})$.

Hidden chemoattractant

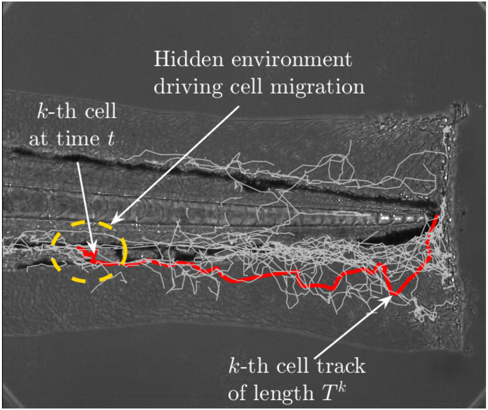

Time series data:

- K tracks: $\mathcal{Y} = \{\mathbf{y}^k\}_{k=1}^{K}$
- Single track: $\mathbf{y}^k = \{\boldsymbol{y}_t^k\}_{t=1}^{T^k}$
- Single data point: $\boldsymbol{y}_t^k = \left[\bar{s}_{\mathrm{x}}, \bar{s}_{\mathrm{y}}\right]^\top$
- Full state: $\boldsymbol{x}_t^k = \left[s_{\mathrm{x}}, s_{\mathrm{y}}, v_{\mathrm{x}}, v_{\mathrm{y}}\right]^\top$
- Environment influence: $\boldsymbol{u}_t^k = \boldsymbol{u}_t^k(\boldsymbol{s}) = \nabla\mathcal{U}(\boldsymbol{s})$.

1. Develop a parametrised finite-order model of global $\mathcal{U}(\boldsymbol{s})$.

Hidden chemoattractant

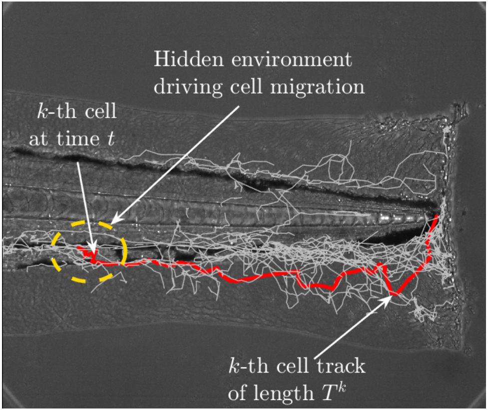

Time series data:

- K tracks: $\mathcal{Y} = \{\mathbf{y}^k\}_{k=1}^K$
- Single track: $\mathbf{y}^k = \{\boldsymbol{y}_t^k\}_{t=1}^{T^k}$
- Single data point: $\boldsymbol{y}_t^k = \left[\bar{s}_{\mathrm{x}}, \bar{s}_{\mathrm{y}}\right]^\top$
- Full state: $\boldsymbol{x}_t^k = \left[s_{\mathrm{x}}, s_{\mathrm{y}}, v_{\mathrm{x}}, v_{\mathrm{y}}\right]^\top$
- Environment influence: $\boldsymbol{u}_t^k = \boldsymbol{u}_t^k(\boldsymbol{s}) = \nabla\mathcal{U}(\boldsymbol{s})$.

1. Develop a parametrised finite-order model of global $\mathcal{U}(\boldsymbol{s})$.
2. Estimate unobserved $\mathcal{U}(\boldsymbol{s})$ from localised tracking data $\mathcal{Y}$.

Defining assumptions

- A migrating call is moving as a massive Brownian particle:

$$\dot{v}(t) = -\rho v(t) + \sqrt{\sigma}\mathbf{W}(t).$$

- Each cell at each time is moving in response to the acting environment:

$$\dot{v}(t) = -\rho v(t) + \sqrt{\sigma}\mathbf{W}(t) + \psi(t).$$

- Hidden chemoattractant environment is acting on cells as a potential field:

$$\dot{v}(t) = -\rho v(t) + \sqrt{\sigma}\mathbf{W}(t) + \nabla\mathcal{U}(s(t)).$$

- Hidden chemoattractant environment is time-invariant:

$$\mathcal{U}(t) = const.$$

Defining assumptions

- A migrating call is moving as a massive Brownian particle:

$$\dot{v}(t) = -\rho v(t) + \sqrt{\sigma}\mathbf{W}(t).$$

- Each cell at each time is moving in response to the acting environment:

$$\dot{v}(t) = -\rho v(t) + \sqrt{\sigma}\mathbf{W}(t) + \psi(t).$$

- Hidden chemoattractant environment is acting on cells as a potential field:

$$\dot{v}(t) = -\rho v(t) + \sqrt{\sigma}\mathbf{W}(t) + \nabla\mathcal{U}(s(t)).$$

- Hidden chemoattractant environment is time-invariant:

$$\mathcal{U}(t) = const.$$

Defining assumptions

- A migrating call is moving as a massive Brownian particle:

$$\dot{v}(t) = -\rho v(t) + \sqrt{\sigma}\mathbf{W}(t).$$

- Each cell at each time is moving in response to the acting environment:

$$\dot{v}(t) = -\rho v(t) + \sqrt{\sigma}\mathbf{W}(t) + \psi(t).$$

- Hidden chemoattractant environment is acting on cells as a potential field:

$$\dot{v}(t) = -\rho v(t) + \sqrt{\sigma}\mathbf{W}(t) + \nabla\mathcal{U}(s(t)).$$

- Hidden chemoattractant environment is time-invariant:

$$\mathcal{U}(t) = const.$$

Defining assumptions

- A migrating call is moving as a massive Brownian particle:

$$\dot{v}(t) = -\rho v(t) + \sqrt{\sigma}\mathbf{W}(t).$$

- Each cell at each time is moving in response to the acting environment:

$$\dot{v}(t) = -\rho v(t) + \sqrt{\sigma}\mathbf{W}(t) + \psi(t).$$

- Hidden chemoattractant environment is acting on cells as a potential field:

$$\dot{v}(t) = -\rho v(t) + \sqrt{\sigma}\mathbf{W}(t) + \nabla\mathcal{U}(s(t)).$$

- Hidden chemoattractant environment is time-invariant:

$$\mathcal{U}(t) = const.$$

Decomposition of the environment

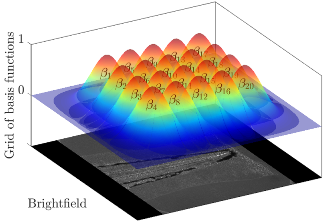

a) 5x4 grid of tensor B-splines

$$\mathcal{U}(s_{\mathrm{x}}, s_{\mathrm{y}}) = \mathcal{B}\Theta = \sum_{h=1}^{N_b} \beta_h(s_{\mathrm{x}}, s_{\mathrm{y}})\theta_h,$$

$$\begin{aligned} \Theta &= [\theta_1, \ldots, \theta_h, \ldots, \theta_{N_b}]^\top, \\ \mathcal{B} &= [\beta_1, \ldots, \beta_h, \ldots, \beta_{N_b}], \\ \beta_h(s_{\mathrm{x}}, s_{\mathrm{y}}) &= \beta_l^4(s_{\mathrm{x}})\beta_m^4(s_{\mathrm{y}}). \end{aligned}$$

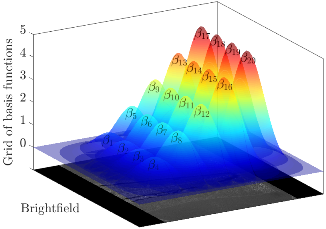

b) θ_h defines magnitude of $\beta_h(s_{\mathrm{x}}, s_{\mathrm{y}})$

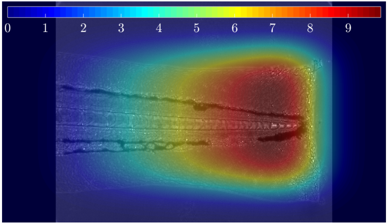

Example of the resultant field.

Decomposition of the environment

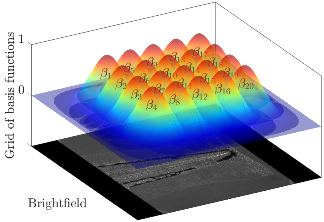

a) 5x4 grid of tensor B-splines

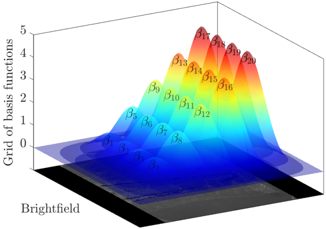

b) θ_h defines magnitude of $\beta_h(s_\mathrm{x}, s_\mathrm{y})$

$$\mathcal{U}(s_\mathrm{x}, s_\mathrm{y}) = \mathcal{B}\Theta = \sum_{h=1}^{N_b} \beta_h(s_\mathrm{x}, s_\mathrm{y})\theta_h,$$

$$\begin{aligned} \Theta &= [\theta_1, \ldots, \theta_h, \ldots, \theta_{N_b}]^\top, \\ \mathcal{B} &= [\beta_1, \ldots, \beta_h, \ldots, \beta_{N_b}], \\ \beta_h(s_\mathrm{x}, s_\mathrm{y}) &= \beta_l^4(s_\mathrm{x})\beta_m^4(s_\mathrm{y}). \end{aligned}$$

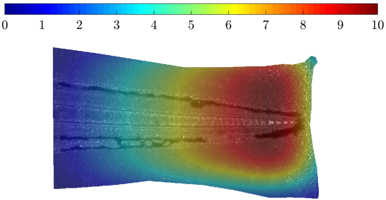

Example of the resultant field.

Model of neutrophil dynamics

Discrete time SSM of the k-th cell :

$$\boldsymbol{x}_{\mathrm{t}}^{\mathrm{k}} = A\boldsymbol{x}_{\mathrm{t}-1}^{\mathrm{k}} + B\phi_{\mathrm{t}-1}^{\mathrm{k}}(s_{\mathrm{x}}, s_{\mathrm{y}})\Theta + G\boldsymbol{w}_{\mathrm{t}-1}^{\mathrm{k}}, \quad \boldsymbol{w}_{\mathrm{t}}^{\mathrm{k}} \sim \mathcal{N}(0, Q)$$

$$\boldsymbol{y}_{\mathrm{t}}^{\mathrm{k}} = C\boldsymbol{x}_{\mathrm{t}}^{\mathrm{k}} + \boldsymbol{v}_{\mathrm{t}}^{\mathrm{k}}, \quad \boldsymbol{v}_{\mathrm{t}}^{\mathrm{k}} \sim \mathcal{N}(0, R)$$

where

$$\phi_{\mathrm{t}}^{\mathrm{k}}(s_{\mathrm{x}}, s_{\mathrm{y}}) = \nabla\mathcal{B}(s_{\mathrm{x}}, s_{\mathrm{y}}) = \begin{bmatrix} \frac{\partial\beta_1(s_{\mathrm{x}}, s_{\mathrm{y}})}{\partial s_{\mathrm{x}}} & \cdots & \frac{\partial\beta_h(s_{\mathrm{x}}, s_{\mathrm{y}})}{\partial s_{\mathrm{x}}} & \cdots & \frac{\partial\beta_{N_b}(s_{\mathrm{x}}, s_{\mathrm{y}})}{\partial s_{\mathrm{x}}} \\ \frac{\partial\beta_1(s_{\mathrm{x}}, s_{\mathrm{y}})}{\partial s_{\mathrm{y}}} & \cdots & \frac{\partial\beta_h(s_{\mathrm{x}}, s_{\mathrm{y}})}{\partial s_{\mathrm{y}}} & \cdots & \frac{\partial\beta_{N_b}(s_{\mathrm{x}}, s_{\mathrm{y}})}{\partial s_{\mathrm{y}}} \end{bmatrix}.$$

$$A = \begin{bmatrix} \mathbb{I} & T\,\mathbb{I} \\ \mathbb{O} & (1 - T\rho)\,\mathbb{I} \end{bmatrix}; B = \begin{bmatrix} \mathbb{O} \\ T\,\mathbb{I} \end{bmatrix}; G = \begin{bmatrix} \mathbb{O} \\ T\,\mathbb{I} \end{bmatrix}; C = \begin{bmatrix} \mathbb{I} & \mathbb{O} \end{bmatrix}.$$

SMM is linear in Θ and non-linear in $\boldsymbol{x}$.

Approximate ML estimation

E-step:

$$\mathcal{Q}(\Theta, \hat{\Theta}^i) = \mathbb{E}\left[\log p(\Theta \mid \mathcal{Y})\right] = \mathbb{E}\left[\sum_{\mathrm{k}=1}^{\mathrm{K}} \sum_{\mathrm{t}=1}^{\mathrm{T_k}} \log p(\boldsymbol{x}_{\mathrm{t}}^{\mathrm{k}} \mid \boldsymbol{x}_{\mathrm{t}-1}^{\mathrm{k}}, \Theta) \mid \mathcal{Y}, \hat{\Theta}^i\right] + c.$$

$$p(\boldsymbol{x}_{\mathrm{t}}^{\mathrm{k}} \mid \boldsymbol{x}_{\mathrm{t}-1}^{\mathrm{k}} \Theta) = \mathcal{N}\left((G)^{\dagger}\left\{\boldsymbol{x}_{\mathrm{t}}^{\mathrm{k}} - A\boldsymbol{x}_{\mathrm{t}-1}^{\mathrm{k}} - B\phi(C\boldsymbol{x}_{\mathrm{t}-1}^{\mathrm{k}})\Theta\right\}, \Sigma_{\boldsymbol{w}}{}^{1}\right).$$

Forecasting step:

$$\boldsymbol{s}_{\mathrm{t}}^{\mathrm{k}} = C\hat{\boldsymbol{x}}_{\mathrm{t}|\mathrm{T}^{\mathrm{k}}}^{\mathrm{k}}, \quad \mathrm{t} = 1, \ldots, \mathrm{T}^{\mathrm{k}}, \mathrm{k} = 1, \ldots, \mathrm{K}.$$

$$\begin{aligned} p(\boldsymbol{x}_{\mathrm{t}}^{\mathrm{k}} \mid \boldsymbol{x}_{\mathrm{t}-1}^{\mathrm{k}}, \Theta) &\approx p(\boldsymbol{x}_{\mathrm{t}}^{\mathrm{k}} \mid \boldsymbol{x}_{\mathrm{t}-1}^{\mathrm{k}}, \boldsymbol{s}_{\mathrm{t}-1}^{\mathrm{k}}, \Theta) \\ &= \mathcal{N}\left((G)^{\dagger}\left\{\boldsymbol{x}_{\mathrm{t}}^{\mathrm{k}} - A\boldsymbol{x}_{\mathrm{t}-1}^{\mathrm{k}} - B\phi(\boldsymbol{s}_{\mathrm{t}-1}^{\mathrm{k}})\Theta\right\}, \Sigma_{\boldsymbol{w}}\right). \end{aligned}$$

M-step:

$$\hat{\Theta}^{i+1} = \arg\max_{\Theta} \tilde{\mathcal{Q}}(\Theta, \hat{\Theta}^i).$$

[1] $\Sigma_{\boldsymbol{w}} \triangleq \left\{(G)^{\dagger}\right\}^{\top}(Q_{\omega})^{-1}(G)^{\dagger}$

Inferred chemoattractant concentration

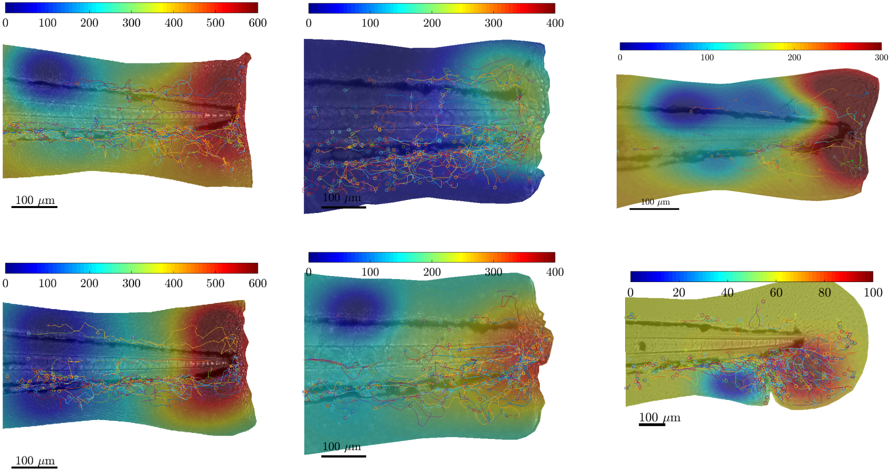

a) normal injury (6 datasets)

b) severe injury (2 datasets)

c) mild injury (6 datasets)

Estimated cell velocities

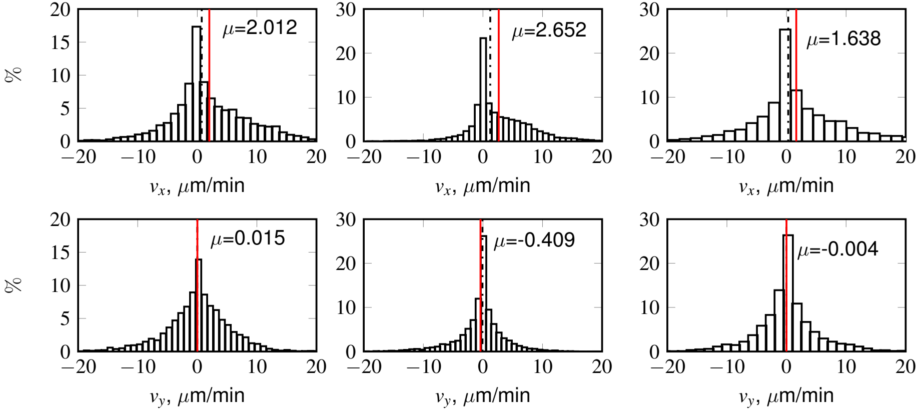

a) normal injury b) severe injury c) mild injury

Heterogeneous cell behaviour

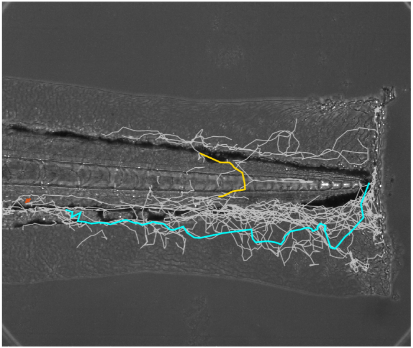

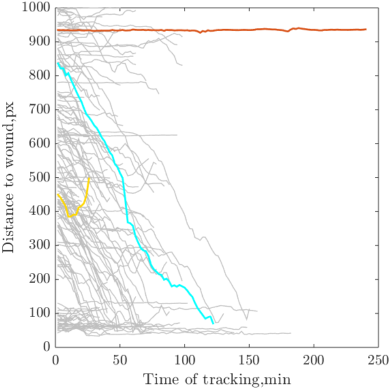

Heterogeneous cell behaviour

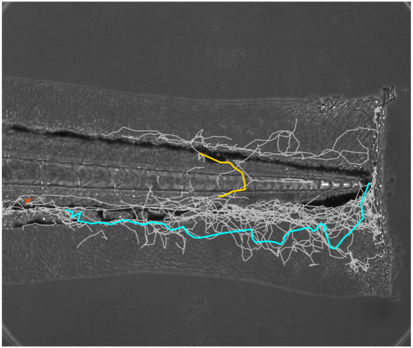

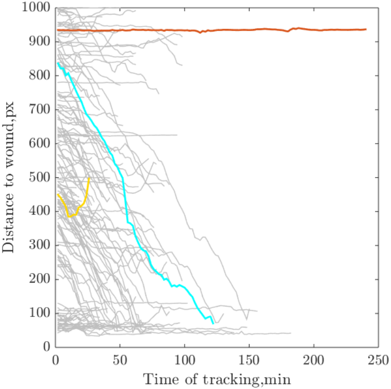

1. Determine whether a cell at a given time interacts with the environment $\mathcal{U}(s)$.

Heterogeneous cell behaviour

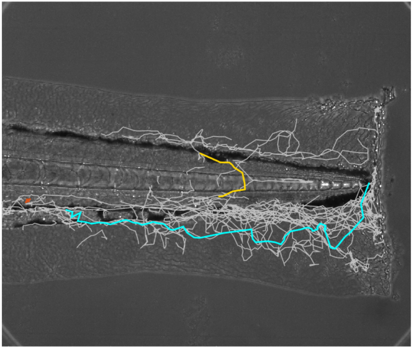

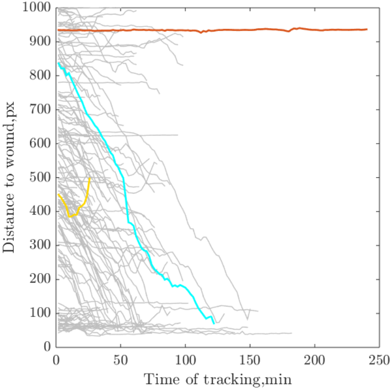

1. Determine whether a cell at a given time interacts with the environment $\mathcal{U}(s)$.
2. Estimate unobserved $\mathcal{U}(s)$ from the interaction with responsive cells.

Defining assumptions (upd.)

Remain the same:

- Each migrating call is moving as a massive Brownian particle.
- Hidden chemoattractant environment is acting on migrating cells as a potential field.
- Hidden chemoattractant environment is time-invariant.

Relaxed assumptions:

- Each migrating cell at any time can be in one of free modes: stationary, responsive or non-responsive.
- Switching between modes happens randomly.
- Each behavioural mode can be reached from any other mode.

Jump Markov system

$$
\begin{aligned}
\boldsymbol{x}_{\mathrm{t}}^{\mathrm{k}} &= A(\boldsymbol{m}_{\mathrm{t}}^{\mathrm{k}})\boldsymbol{x}_{\mathrm{t}-1}^{\mathrm{k}} + B(\boldsymbol{m}_{\mathrm{t}}^{\mathrm{k}})\phi_{\mathrm{t}-1}^{\mathrm{k}}(s_{\mathrm{x}}, s_{\mathrm{y}})\Theta + G(\boldsymbol{m}_{\mathrm{t}}^{\mathrm{k}})\boldsymbol{w}_{\mathrm{t}-1}^{\mathrm{k}},\\
\boldsymbol{w}_{\mathrm{t}}^{\mathrm{k}} &\sim \mathcal{N}(0, Q(\boldsymbol{m}_{\mathrm{t}}^{\mathrm{k}})),\\
\boldsymbol{m}_{\mathrm{t}}^{\mathrm{k}} &\in \left\{M^1, M^2, M^3\right\}.
\end{aligned}
$$

Cell modes:

$$M^1 : A = \begin{bmatrix} \mathbb{I} & T\,\mathbb{I} \\ \mathbb{O} & (1 - T\rho(M^1))\,\mathbb{I} \end{bmatrix} B = \begin{bmatrix} \mathbb{O} \\ T\,\mathbb{I} \end{bmatrix}$$

$$M^2 : A = \begin{bmatrix} \mathbb{I} & T\,\mathbb{I} \\ \mathbb{O} & (1 - T\rho(M^2))\,\mathbb{I} \end{bmatrix} B = \begin{bmatrix} \mathbb{O} \\ \mathbb{O} \end{bmatrix}$$

$$M^3 : A = \begin{bmatrix} \mathbb{I} & T\,\mathbb{I} \\ \mathbb{O} & (1 - T\rho(M^3))\,\mathbb{I} \end{bmatrix} B = \begin{bmatrix} \mathbb{O} \\ \mathbb{O} \end{bmatrix}$$

$$Q(M^3) \ll Q(M^1) < Q(M^2).$$

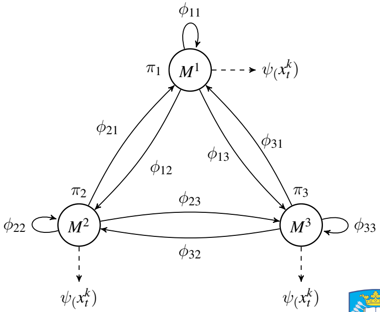

Inference framework

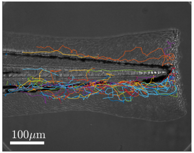

$\{M^1, M^2, M^3\}$

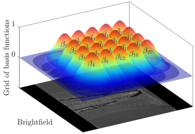

Approximate ML framework

MM smoother
$\mathcal{X}, \mathcal{M} \mid \hat{\Theta}^i$

Forecasting
$\mathcal{S} \mid \mathcal{X}, \hat{\Theta}^i$

$$\hat{\Theta}^{i+1} = \arg\max_{\Theta} \tilde{\mathcal{Q}}(\mathcal{X}, \mathcal{M}, \mathcal{S})$$

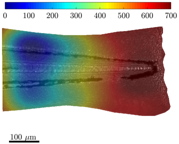

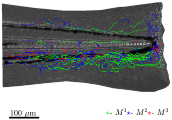

Inference framework

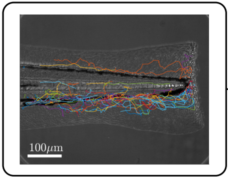

$$\{M^1, M^2, M^3\}$$

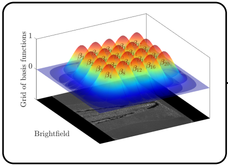

Approximate ML framework

MM smoother

$$\mathcal{X}, \mathcal{M} \mid \hat{\Theta}^i$$

Forecasting

$$\mathcal{S} \mid \mathcal{X}, \hat{\Theta}^i$$

$$\hat{\Theta}^{i+1} = \arg\max_{\Theta} \tilde{\mathcal{Q}}(\mathcal{X}, \mathcal{M}, \mathcal{S})$$

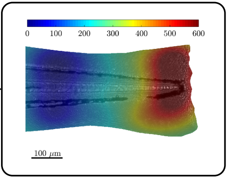

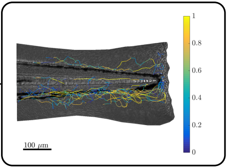

Migratory modes - normal injury

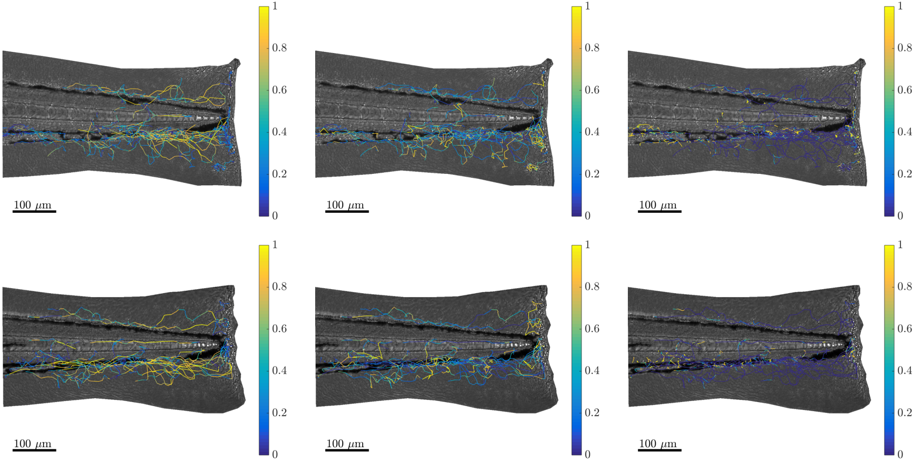

a) $p(M^1)$ b) $p(M^2)$ c) $p(M^3)$

Migratory modes - severe and mild injury

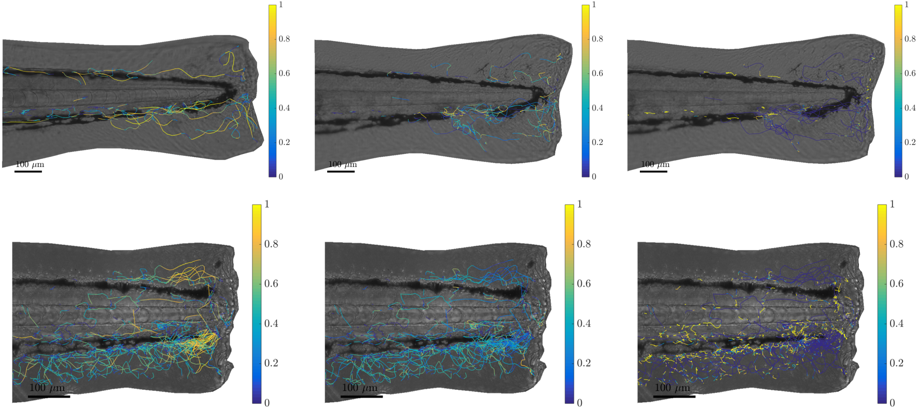

a) $p(M^1)$ b) $p(M^2)$ c) $p(M^3)$

Inferred chemoattractant environment

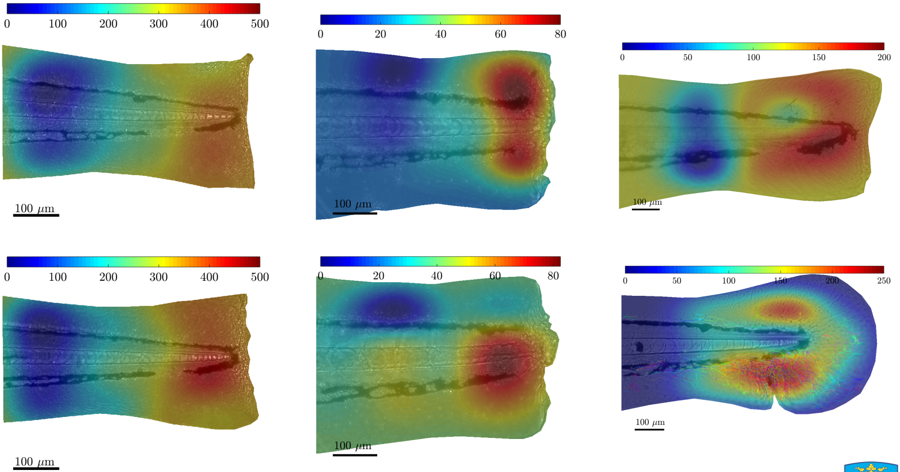

a) normal injury b) severe injury c) mild injury

Reverse migration

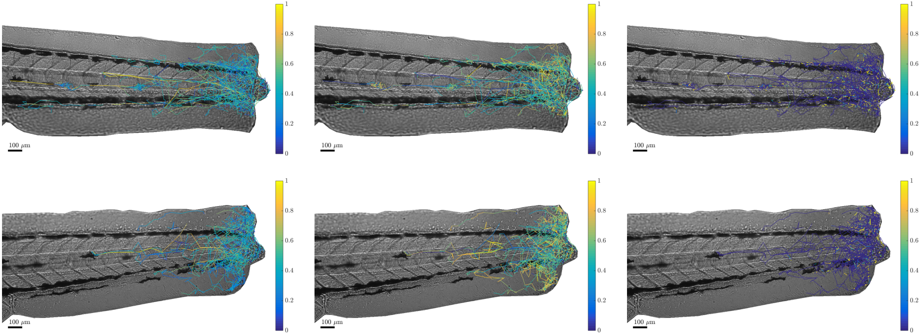

a) $p(M^1)$ b) $p(M^2)$ c) $p(M^3)$

For 4 datasets there is higher probability of neutrophils diffusing away from the wound.

Signal to migration

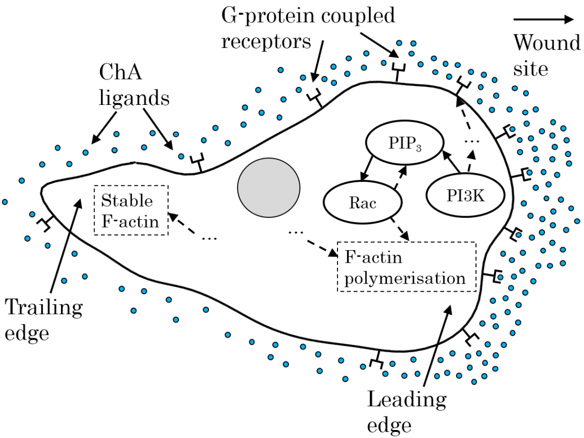

Signal to migration

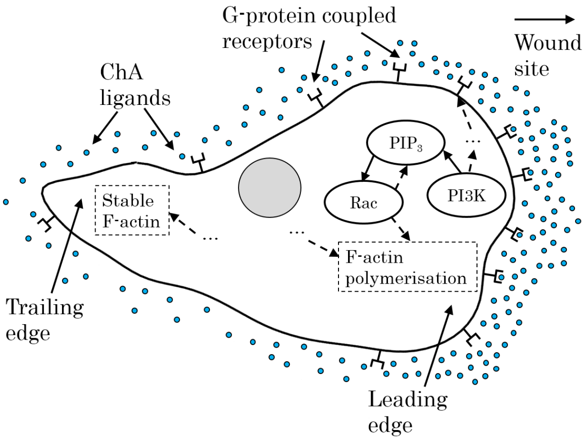

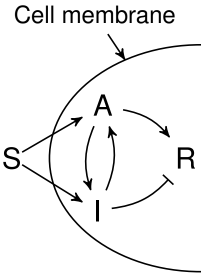

Signal to migration

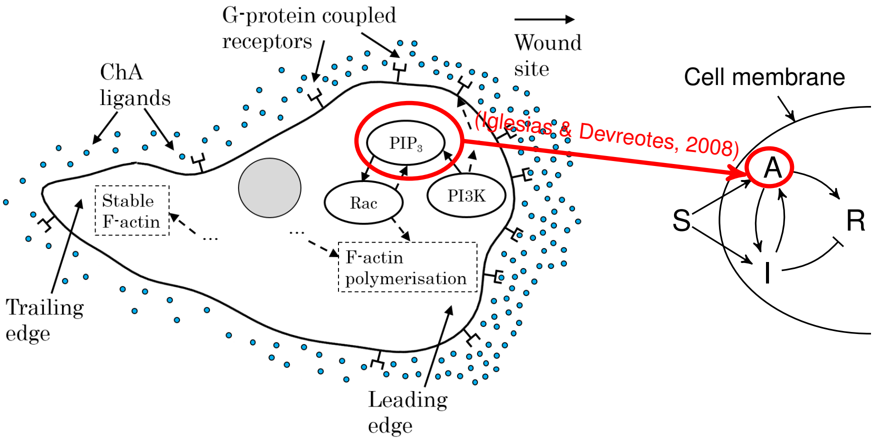

Signal to migration

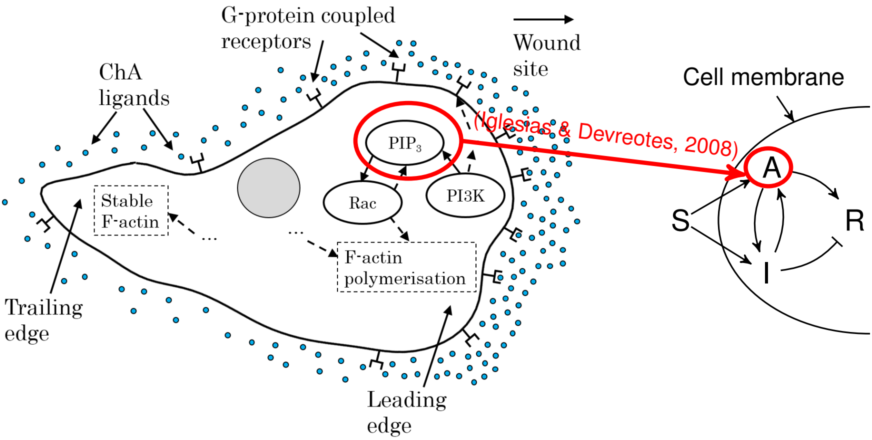

Does PIP$_3$ activate pseudopod growth in migrating neutrophils?

Data

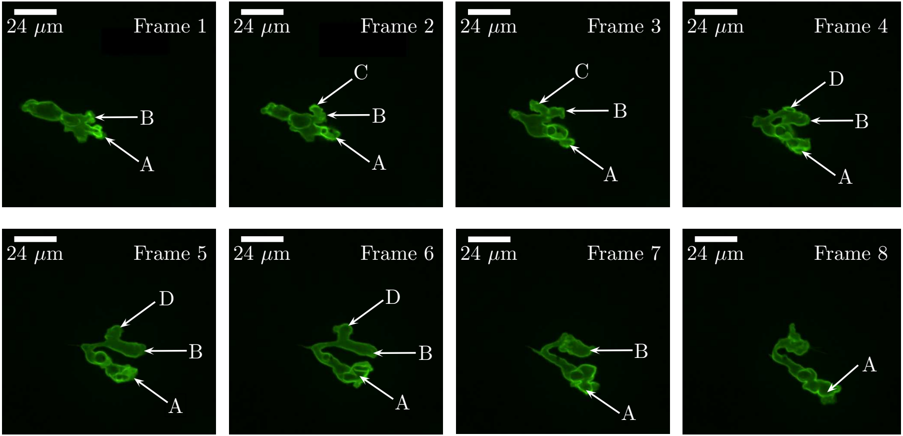
24 μm
Frame 1
B
A
24 μm
Frame 2
C
B
A
24 μm
Frame 3
C
B
A
24 μm
Frame 4
D
B
A
24 μm
Frame 5
D
B
A
24 μm
Frame 6
D
B
A
24 μm
Frame 7
B
A
24 μm
Frame 8
A

Defining assumptions

- PIP_3 is the only activator regulating cell membrane protrusions.
- The integrated fluorescence intensity obtained from the imaging data is proportional to the local PIP_3 concentration.
- The cell is a 2-D curve Γ_{t}.
- Local shape change is fully described by the evolution of local normal velocity.

$$\boldsymbol{v}_{\mathrm{t}+1}^{k} = \boldsymbol{v}_{\mathrm{t}}^{k} + \frac{1}{m}\mathcal{F} + \boldsymbol{w}_{\mathrm{t}}.$$

Forces acting on cell boundary

$$\mathcal{F} = (\mathcal{F}_{\text{visc}} + \mathcal{F}_{\text{pro}} + \mathcal{F}_{\text{ten}} + \mathcal{F}_{\text{vol}})\nu,$$

- ***Protrusive force*** caused by acting regulators along the membrane:

$$\mathcal{F}_{\text{pro}} = \alpha_{\text{pro}} a_{\text{t}}^{k}.$$

- ***Surface tension*** prevents cell membrane from stretching:

$$\mathcal{F}_{\text{ten}} = \alpha_{\text{ten}} \kappa_{\text{t}}^{k}.$$

- ***Volume conservation*** balances small volume changes:

$$\mathcal{F}_{\text{vol}} = \alpha_{\text{vol}} \Delta \mathcal{A}_{\text{t}}.$$

- ***Viscous force*** opposes cell motion:

$$\mathcal{F}_{\text{visc}} = -\alpha_{\text{vv}} \boldsymbol{v}_{\text{t}}^{k}.$$

State space model

$$\Gamma_{\mathrm{t}} : \mathrm{s}_{\mathrm{t}}^k, \quad k = 1, \ldots, K.$$

Local evolution for the node $\mathrm{s}_{\mathrm{t}}^k$:

$$\boldsymbol{v}_{\mathrm{t}+1}^k = A\boldsymbol{v}_{\mathrm{t}}^k + \boldsymbol{B}\boldsymbol{u}_{\mathrm{t}}^k + \boldsymbol{w}_{\mathrm{t}}^k, \quad \boldsymbol{w}\mathrm{t}^k \sim \mathcal{N}(0, Q).$$

$$\boldsymbol{y}_{\mathrm{t}}^k = C\boldsymbol{v}_{\mathrm{t}}^k.$$

- $A = 1 - \alpha_{\mathrm{vv}}$; $B = \left[\alpha_{\mathrm{pro}}, \alpha_{\mathrm{ten}}, \alpha_{\mathrm{vol}}\right]$;
- $\boldsymbol{u}_{\mathrm{t}}^k = \left[a_{\mathrm{t}}^k, \kappa_{\mathrm{t}}^k, \Delta\mathcal{A}_{\mathrm{t}}\right]^\top$, where
  - a_{t}^k - local concentration of PIP_3;
  - κ_{t}^k - local curvature;
  - $\Delta\mathcal{A}_{\mathrm{t}} = \mathcal{A}_{\mathrm{t}} - \mathcal{A}_0$ - change in cell shape.
- $\Theta = \{A, B, Q, \boldsymbol{v}_0, P_0\}$ - estimated via classic EM algorithm.

Image processing

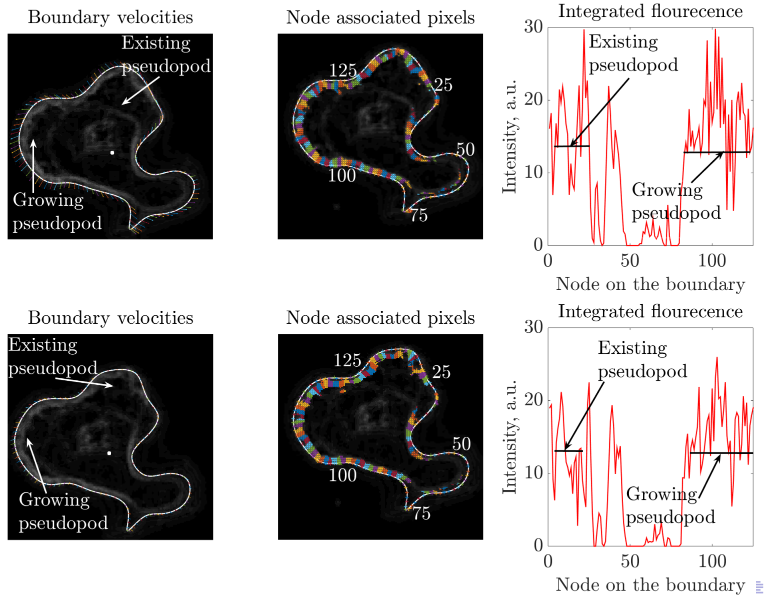

Motile cells observed in vivo

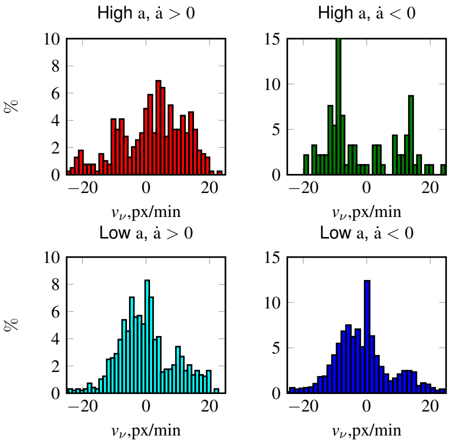

- Very weak correlation between between a^k_{t-1} and v^k_t for all cells;
- PIP_3 does not activate protrusion growth;
- Mann-Whitney test results: on average, higher concentrations of PIP_3 accelerate protrusion growth.

Motile cells observed in vivo

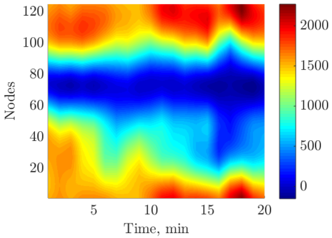

a) Smoothed intensity.

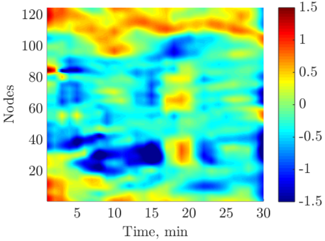

c) Estimated velocity.

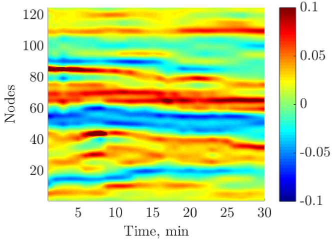

a) Local curvature.

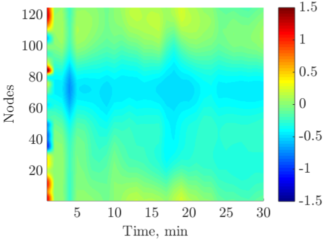

d) Predicted velocity.

Polarised cell observed in vitro

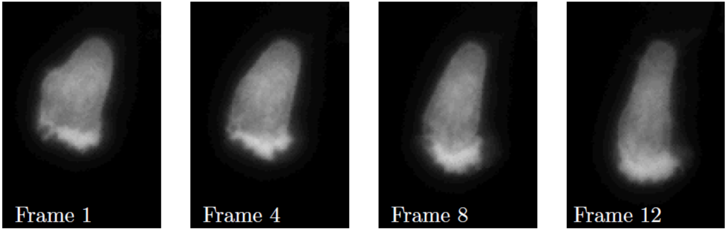

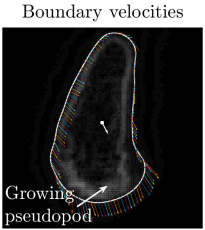

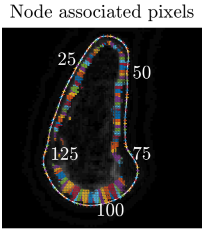

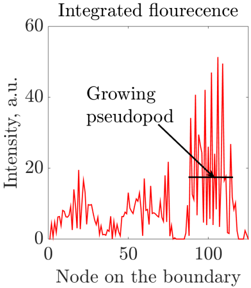

Polarised cell observed in vitro

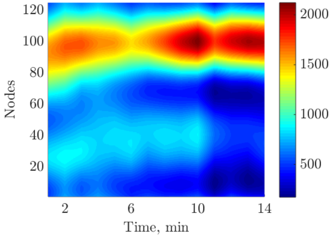

a) Smoothed intensity.

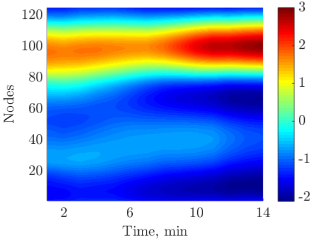

c) Estimated velocity.

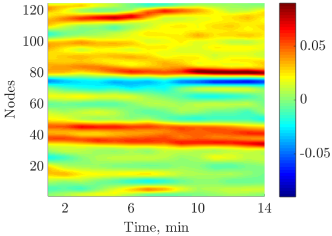

a) Local curvature.

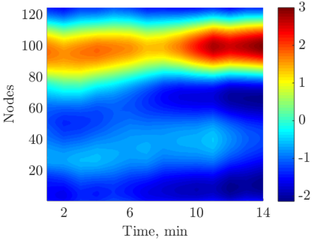

d) Predicted velocity.

Technical contributions

- A reconfigurable hybrid model of individual cell dynamics that incorporates the influence of the global environment.
- A statistical framework for simultaneous inference of the global chemoattractant environment and cell behavioural modes.
- An image processing and estimation framework that links local cell boundary evolution to observed subcellular concentrations.

Contributions in field of application

- Investigation of neutrophil-environment interaction on different stages of inflammation.
- Quantitative evidence that the dominant mode of neutrophil reverse migration is random walk.
- Quantitative evidence that PIP_3 does not activate protrusions but accelerates existing leading edges in cells performing chemotaxis.

Future work

- Utilising hierarchical/multi-resolution basis functions in environment decomposition.
- Introducing priors for the field parameters and Bayesian inference.
- Considering time-varying environment for recruitment stage of inflammation.
- Considering competing gradients for resolution stage of inflammation.
- Shorten this presentation.

Disseminated results

- A. Kadochnikova, H.M. Isles, S.A. Renshaw, V. Kadirkamanathan. "Estimation of Hidden Chemoattractant Field from Observed Cell Migration Patterns". A peer-reviewed paper in *Proceedings of 18th IFAC Symposium on System Identification SYSID 2018*.
- H.M. Isles, C. Muir, A. Kadochnikova, C.A. Loynes, V. Kadirkamanathan, P.M. Elks, S.A. Renshaw. "Non-apoptotic pioneer neutrophils initiate a swarming response in a zebrafish tissue injury model" under review in eLife Reports, 2019.

In preparation:

- A. Kadochnikova, V. Kadirkamanathan. "An Approximate Maximum Likelihood Framework for Estimating the Environment Driving multiple objects with Hybrid Dynamics".
- A. Kadochnikova, H.M. Isles, S.A. Renshaw, V. Kadirkamanathan. "Inference of the External Stimuli Environments from Heterogeneous Behaviour of Migrating Neutrophils in Zebrafish Model of Inflammation".

Thank you!
Questions?